Emission of Nonclassical Radiation by Inelastic Cooper Pair Tunneling

M. Westig,[1] B. Kubala,[2] O. Parlavecchio,[1] Y. Mukharsky,[1] C. Altimiras,[1] P. Joyez,[1] D. Vion,[1] P. Roche,[1] D. Esteve,[1] M. Hofheinz,[1,*] M. Trif,[3] P. Simon,[3] J. Ankerhold,[2,†] and F. Portier[1,‡]

[1]*SPEC, CEA, CNRS, Université Paris-Saclay, CEA Saclay, 91191 Gif-sur-Yvette, France*

[2]*Institute for Complex Quantum Systems and IQST, University of Ulm, 89069 Ulm, Germany*

[3]*Laboratoire de Physique des Solides, Université Paris-Sud, 91405 Orsay, France*

(Received 21 March 2017; published 26 September 2017)

We show that a properly dc-biased Josephson junction in series with two microwave resonators of different frequencies emits photon pairs in the resonators. By measuring auto- and intercorrelations of the power leaking out of the resonators, we demonstrate two-mode amplitude squeezing below the classical limit. This nonclassical microwave light emission is found to be in quantitative agreement with our theoretical predictions, up to an emission rate of 2 billion photon pairs per second.

DOI: 10.1103/PhysRevLett.119.137001

Microwave radiation is usually produced by ac driving a conductor like a wire antenna. The radiated field is then a so-called coherent state [1] that closely resembles a classical state. On the other hand, a simply dc-biased quantum conductor can also generate microwave radiation, owing to the probabilistic nature of the discrete charge transfer through the conductor, which causes quantum fluctuations of the current [2–4]. Coupled to a resonant mode, this stochastic emission can lead to masing [5–9]. More generally, it is expected that the quantum character of the charge transfer may imprint in the properties of the emitted radiation, possibly leading to nonclassical radiation, such as, e.g., antibunched photons [10–17]. One may wonder what other types of interesting or useful nonclassical states of light can be generated with such a simple method. In this Letter, we investigate the properties of photon pairs emitted by a dc voltage-biased Josephson junction. In such a junction, at bias voltage less than the gap voltage $2\Delta/e$, no quasiparticle excitation can be created in the superconducting electrodes. Thus, a dc current can only flow through the junction when the electrostatic energy $2eV$ associated to transfer of the charge of a Cooper pair through the circuit is absorbed by modes of the surrounding circuit [18–23].

In order to obtain a situation in which the quantum nature of the emitted radiation can be probed quantitatively, we place such a dc-biased Josephson junction in an engineered environment made of two series resonators with different frequencies ν_a, ν_b, as shown in Fig. 1(a). We consider, in particular, the resonance condition $2eV = h(\nu_a + \nu_b)$, at which the transfer of a single Cooper pair is expected to create one photon in each resonator, leaking afterwards in two microwave lines. By measuring both photon emission rates as well as the power-power auto- and intercorrelations, we prove that these correlations violate a Cauchy-Schwartz inequality obeyed by classical light, meaning that the relative fluctuations of the outgoing modes are suppressed below the classical limit. This two-mode amplitude squeezing is observed for emission rates as high as 2×10^9 photon pairs per second, making our setup a particularly bright (and simple) source of nonclassical radiation.

Our experimental setup is shown in Fig. 1(b): a superconducting quantum interference device (SQUID) acts as a tunable Josephson junction with Josephson energy $E_J = E_{J0}|\cos(2e\Phi/\hbar)|$ adjustable via the magnetic flux Φ threading its loop. The two resonators galvanically coupled to either side of the SQUID are made of three cascaded quarter-wave transformers. Their expected fundamental modes have frequencies $\nu_{a,b} \simeq 4.9, 6.7$ GHz and characteristic impedances $Z_{a,b} \simeq 140\ \Omega$. Cooper pairs tunneling through the SQUID induce current fluctuations through the inner conductors of the quarter-wave transformers, and can thus excite the resonators. The resonators connect to two separate bias tees, making it possible to dc voltage bias the SQUID while collecting radiation on two separate microwave lines with wave impedance $50\ \Omega$. The resonator quality factors $Q_{a,b} \simeq 25, 35$ are thus determined by the energy leaking rate $\kappa_{a,b} \simeq 1.3 \times 10^9\ \mathrm{s}^{-1}$ into each microwave line. The expected total series impedance $Z(\nu)$ seen by the SQUID thus reaches $\simeq$3.2, 4.9 kΩ for modes a and b. The two measurement lines are arranged in a Hanbury Brown–Twiss (HBT) microwave setup to probe the quantum fluctuations of the emitted radiation without being blinded by the noise of the amplification chains: they are connected through two isolators to a 90° hybrid coupler acting as a microwave beam splitter. The two lines after the coupler (hereafter called 1 and 2) thus propagate half of the powers leaking from resonators a and b. The two outputs of the beam splitter are sent through two additional isolators and filters to two microwave high-electron-mobility transistor (HEMT) amplifiers placed at 4.2 K. These isolators and filters protect the sample from the amplifiers' back-action noise and ensure thermalization of its environment

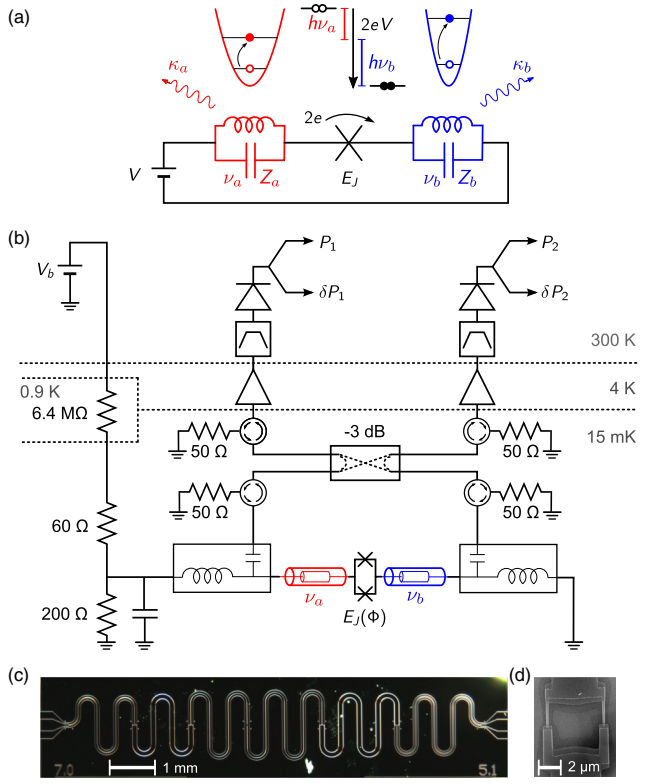

FIG. 1. Principle and setup of the experiment. (a) A Josephson junction in series with two resonators with frequencies $\nu_{a,b}$ emits a photon pair in the resonators each time a Cooper pair tunnels through it at a dc bias voltage V such that $2eV = h\nu_a + h\nu_b$. Microwave radiations leaking out of the resonators at rates $\kappa_{a,b}$ should present strong quantum correlations. (b) Setup: The sample consists of a SQUID [SEM micrograph shown in (d)] working as a magnetically tunable Josephson junction in series with two three-quarter-wave transformer resonators whose optical micrograph is shown in (c). Two bias tees make it possible to dc voltage bias the SQUID while collecting radiation from the resonators. A HBT setup with a hybrid coupler, isolators, amplifiers, filters, and power detectors is used to measure all powers and power-power correlations (see the text).

during the experiment. They also attenuate the signals by about 3 dB. After further amplification at room temperature [not shown in Fig. 1(b)], the signals are filtered either by a heterodyne technique implementing a 12 MHz-wide bandpass filter at tunable frequency or by adjustable bandpass cavity filters covering only one of the resonator lines. In both cases, the filtered signal is detected by a quadratic detector, whose output voltage is proportional to its input ac power $P_{1,2}(t)$. In order to extract the small average contribution $\langle P^S_{1,2}\rangle$ of the sample from the large background noise of the cryogenic amplifiers, we apply a 0 to V square-wave modulation at 113 Hz to the sample bias and perform a lock-in detection of the square-wave response of the quadratic detectors.

The sample is cooled to 15 mK in a dilution refrigerator. We first characterize *in situ* our sample and detection chain using the quasiparticle shot noise as a calibrated source [22]: We measure the power emitted by the SQUID at bias voltage $V \simeq 0.975$ mV, well above the gap voltage $2\Delta/e \simeq 0.4$ mV. Under these conditions, the voltage derivative of the measured power spectral density reads $2e\mathrm{Re}Z(\nu)R_n/|R_n + Z(\nu)|^2 \times G$ with $R_n = 8.0$ kΩ being the tunnel resistance of the SQUID in the normal state, and G the total gain of the setup. The measured frequency dependence is in good agreement with the above formula, using our design of $Z(\nu)$. This measurement thus provides an *in situ* determination of gain G. More information on the design and comparison with the high bias data can be found in Supplemental Material [24].

We then measure the emitted power spectral density S as a function of frequency and bias voltage for the single photon (left side of Fig. 2) and two-photon emission processes (right side of Fig. 2). To do so, we ensure a maximum population of the resonators of order unity by setting E_J at a sufficiently small value [25]. The single photon processes occur along the $2eV = h\nu$ line, with an intensity modulated by $\mathrm{Re}Z(\nu)$. At fixed bias voltage, the 12 MHz spectral width of the detected radiation coincides with our detection bandwidth, proving that our bias line is well filtered and adds to the Josephson frequency $2eV/h$ an incertitude negligible compared with the width of the resonators $\kappa_{a,b}/2\pi$. Fainter lines appear at $2eV = h(\nu_{a,b} \pm m\nu_P)$, with $\nu_P = 35$ MHz and m being an integer. We attribute these satellite peaks to the existence of a parasitic resonance at frequency ν_P, allowing for multiphoton processes with one photon emitted at high frequency ν_a or ν_b and m photons emitted into or absorbed from the parasitic mode. From the relative weight of the peaks (data not shown here), we estimate the impedance of this parasitic mode to $Z_P = 204$ Ω, with a thermal population of $n_p \sim 8$ photons corresponding to a 14.5 mK temperature for the ν_P mode. This is in good agreement with the measured fridge temperature of 15 ± 1 mK.

At higher bias voltages (right side of Fig. 2) we detect processes for which the tunneling of a Cooper pair is associated to the emission of two photons: At $V = 20.2$ μV (respectively 27.9 μV), we detect radiation around the frequency of resonator a (respectively b) due to the simultaneous emission of two photons into this resonator for each Cooper pair tunneling through the junction. At an intermediate voltage $V = 24.1$ μV, we detect radiation at both frequencies ν_a and ν_b, due to the simultaneous emission of a photon in each resonator for each Cooper pair transferred. The rightmost panel of Fig. 2 shows the corresponding power spectral density of the emitted radiation. Integrating this spectral power over a 500 MHz bandwidth centered around ν_a and ν_b indeed shows that the photon emission rates into resonators a and b coincide (within 10% due to calibration uncertainties). At fixed bias voltage V the spectral width of the emitted radiation from any two photon process is comparable with the width of the

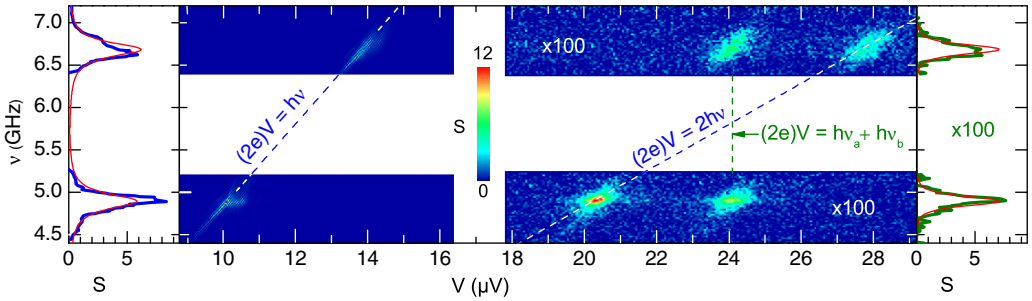

FIG. 2. Detected power spectral density S as a function of frequency ν and dc bias voltage V, reexpressed in terms of photon rate per unit bandwidth at the output of the resonators. Emission occurs at one photon per Cooper pair along the line $2eV = h\nu$ (see left two-dimensional map), and at two identical photons per Cooper pair along the $2eV = 2h\nu$ line and one pair of photons in modes a, b along the vertical line $2eV = h\nu_a + h\nu_b$ (see right two-dimensional map). The leftmost panel is a cut along the $2eV = h\nu$ line showing the emitted power (blue bold line). The rightmost panel is a cut at $V = 24.1\ \mu V = h(\nu_a + \nu_b)/(2e)$. Spectral density for the two-photon processes has been multiplied by 100 for clarity. The red curves show the predictions of the $P(E)$ theory with $E_J = 1.42\ \mu\text{eV} \pm 0.07\ \mu\text{eV}$ being the only adjustable parameter.

resonators: Because of energy conservation, the sum of the frequencies of the two emitted photons is equal to the Josephson frequency $\nu_J = 2eV/h$. As a consequence, if one of the photons is emitted at frequency ν, the other is emitted at frequency $\nu_J - \nu$. The corresponding weight is given by the product of the environment's impedances $\text{Re}[Z(\nu)]\text{Re}[Z(\nu_J - \nu)]/R_Q^2$, and $R_Q = h/4e^2$, resulting in a width of the emitted radiation of the order of half that of the resonator [22].

It is quite intuitive that a common excitation process that creates one photon in each resonator for each Cooper pair tunneling through the junction yields strong nonclassical correlations of the resonators' occupation numbers $n_a = a^\dagger a$ and $n_b = b^\dagger b$. This effect is quantified by the so-called noise reduction factor $\text{NRF} = \text{var}(n_a - n_b)/\langle n_a + n_b\rangle$, i.e., the variance of the occupation difference, normalized to the average total number of photons, yielding 1 in the case of two independent coherent states. With photon pair creation in nonleaking resonators, n_a and n_b remain equal and the NRF is reduced to 0. In reality, due to the uncorrelated energy decays of the two resonators, n_a and n_b do not remain equal, even for perfectly symmetric modes, and the NRF is expected to increase from 0 to 1/2 [26,27].

The NRF can be linked to the zero-delay value of second order coherence functions

$$g^{(2)}_{\alpha,\beta}(\tau) = \frac{\langle \beta^\dagger(0)\alpha^\dagger(\tau)\alpha(\tau)\beta(0)\rangle}{\langle \alpha^\dagger(\tau)\alpha(\tau)\rangle\langle \beta^\dagger(0)\beta(0)\rangle}$$

with $\alpha, \beta \in \{a, b\}$. We get

$$\begin{aligned}\text{NRF} &= 1 + \frac{\langle n_a\rangle^2 g^{(2)}_{a,a}(0) + \langle n_b\rangle^2 g^{(2)}_{b,b}(0) - 2\langle n_a\rangle\langle n_b\rangle g^{(2)}_{a,b}(0)}{\langle n_a + n_b\rangle} \\ &= 1 + \langle n\rangle \frac{g^{(2)}_{a,a}(0) + g^{(2)}_{b,b}(0) - 2g^{(2)}_{a,b}(0)}{2} \qquad (1)\end{aligned}$$

for $\langle n_a\rangle = \langle n_b\rangle = \langle n\rangle$. A classical bound $\text{NRF} \geq 1$ follows from the Cauchy-Schwarz inequality

$$g^{(2)}_{a,b}(0) \leq \frac{g^{(2)}_{a,a}(0) + g^{(2)}_{b,b}(0)}{2}, \qquad (2)$$

valid for two classical fields, i.e., for a two-mode density operator corresponding to any statistical mixture of coherent states. It is easy to explain why the above inequality must be violated in our situation, with hence a NRF below 1: for low Cooper pair tunneling rates, photons have time to leak out of the resonators between each photon pair creation events. The probabilities to simultaneously find two photons in the same mode, as measured by the autocorrelation $g^{(2)}_{\alpha\alpha}(0)$ is then close to 0 while the cross-correlation $g^{(2)}_{ab}(0)$ giving the probability to find simultaneously one photon in each mode is high [28]. This situation corresponds to a squeezing of the relative amplitudes of the two modes below the classical limit [29–32].

To experimentally probe this violation, we collect the photons leaking out into the measurement lines. At the resonator outputs, the three functions $g^{(2)}_{\alpha_L,\beta_L}$, where $\alpha_L = \sqrt{\kappa_\alpha}\alpha$ and $\beta_L = \sqrt{\kappa_\beta}\beta$ are the propagating field operators, are simply equal to $g^{(2)}_{\alpha,\beta}$ inside the resonators. Both propagating fields a_L and b_L are then beam splitted and sent to lines 1 and 2, which include ≃650 MHz-wide filters centered around ν_α and ν_β to select the desired resonator contributions. Measuring the output powers $P_1(t)$ and $P_2(t)$ using two Herotek DTM 180 AA fast quadratic detectors with a 0.42 ± 0.02 ns response time [33], we obtain the correlation functions

$$g^{(2)}_{\alpha,\beta}(\tau) = 1 + \frac{\langle \delta P_1(t+\tau)\delta P_2(t)\rangle}{\langle P_1^S\rangle\langle P_2^S\rangle}, \qquad (3)$$

where $\langle P^S_{1,2}\rangle = \langle P_{1,2}(V,t)\rangle - \langle P_{1,2}(0,t)\rangle$ are the average sample contributions and $\delta P_{1,2}(t) = P_{1,2}(V,t) - \langle P_{1,2}(V,t)\rangle$ are the power fluctuations. The advantage of this strategy is that it gives access to the fluctuations of the power emitted by the sample eliminating parasitic terms due to the much higher noise power of the HEMT amplifiers [34–38]. Figure 3 shows the three coherence functions $g^{(2)}_{\alpha,\beta}$ at zero delay τ as well as the NRF, as a function of the photon pair emission rate Γ, the latter being varied by scanning the flux threading the SQUID loop. The figure shows that inequality (2) is indeed violated for photon emission rates up to 2×10^9 photon pairs per second, the NRF remaining close to 0.7 [39]. The decay of $g^{(2)}_{a,b}(\tau)$ due to the independent resonator leakage is shown in the inset.

To compare our measurements with theory, we compute the $g^{(2)}_{\alpha,\beta}(\tau)$ functions. This task goes beyond the framework of the standard Dynamical Coulomb Blockade theory, which assumes that the electromagnetic environment of the junction remains in equilibrium. Here instead we need to predict how the presence of photons already emitted in the resonators modifies the next emission process. To do so, one can develop an input-output approach [28,40]. Equivalently, we use here a Lindblad master equation approach, starting from the Hamiltonian

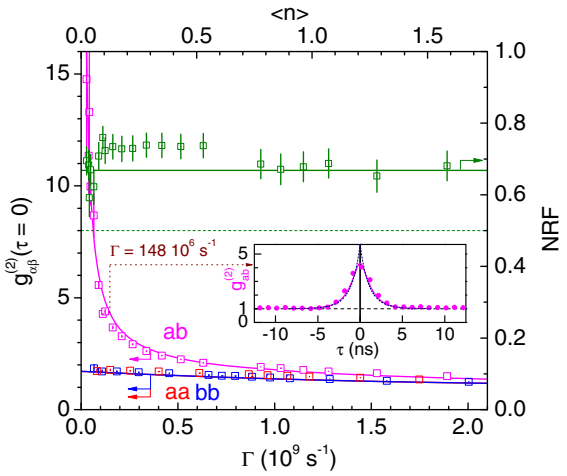

FIG. 3. *Non classicality of the emitted radiation* at bias $V = 24.1\ \mu$V, as a function of the photon pair emission rate. Left scale: Zero delay power-power correlation functions $g^{(2)}_{aa}(0)$ (red open squares), $g^{(2)}_{ab}(0)$ (magenta open squares) and $g^{(2)}_{bb}(0)$ (blue open squares). Right scale: the corresponding NRF (green open squares) extracted from Eq. (1) does not reach the ideal value of 0.5 (horizontal dashed line), but remains well below 1, which demonstrates two-mode amplitude squeezing. Inset: Time dependence of $g^{(2)}_{ab}(\tau)$. The solid lines are theoretical predictions without adjustable parameters. In the inset, the magenta curve includes the effect of the detector finite response time, while the dark blue dashed corresponds to the prediction for infinitely fast detectors.

$$H = h\nu_a a^\dagger a + h\nu_b b^\dagger b - E_J\cos\left[2eVt/\hbar + \Delta_a(a^\dagger + a) + \Delta_b(b^\dagger + b)\right] \quad (4)$$

modeling the two resonators coupled to the voltage biased junction V [15,26,27], with $\Delta_{a,b} = (\pi Z_{a,b}/R_Q)^{1/2}$. Assuming $2eV = h(\nu_a + \nu_b)$ and moving to the frame rotating at $\omega_J = 2eV/\hbar$, the Hamiltonian in the rotating wave approximation then reads

$$H_{\rm RW} = \frac{E_J^*}{2} : \frac{J_1(2\Delta_a\sqrt{a^\dagger a})J_1(2\Delta_b\sqrt{b^\dagger b})}{\sqrt{a^\dagger a}\sqrt{b^\dagger b}}(a^\dagger b^\dagger + ab), \quad (5)$$

with $E_J^* = E_J e^{-(\Delta_a^2+\Delta_b^2)/2}$ being the Josephson energy renormalized by the zero-point fluctuations of the two modes, and the colons characters meaning normal ordering of the operators. The Bessel functions of the first kind J_1 "dress" the elementary photon pair creation process $a^\dagger b^\dagger$ by higher-order corrections in $n_{a,b}$. Note that for low photon numbers $n_{a,b}$ and for low impedances $Z_{a,b} \ll R_Q$, $H_{\rm RW}$ reduces to $H'_{\rm RW} \simeq (E_J^*\Delta_a\Delta_b/2)(a^\dagger b^\dagger + ab)$, which suffices to qualitatively explain the experimental data. Photon leakage from the resonators can be accounted for by including damping rates κ_α of standard quantum-optical form (in the $T = 0$ limit) in the quantum master equation of the system,

$$\dot\rho = -\frac{i}{\hbar}[H_{\rm RW},\rho] + \sum_{\alpha=a,b}\kappa_\alpha(2\alpha\rho\alpha^\dagger - \alpha^\dagger\alpha\rho - \rho\alpha^\dagger\alpha). \quad (6)$$

Additional incoherent dynamics of the a and b modes is caused by the parasitic low frequency mode ν_P [15] and broadens the one-photon resonances. However, we find that it has little impact on the two-photon a-b resonance.

Simulating (6) yields $\rho(t)$ and hence all $g^{(2)}_{\alpha\beta}(\tau)$ functions. These functions, convoluted with the 0.42 ± 0.02 ns detector response mentioned above, are plotted as lines in Fig. 3. They are found in agreement with the experimental results. Note that the deviation from NRF $= 1/2$ seen in Fig. 3 is almost only due to this finite response time. Note also that although the Hamiltonian of Eq. (5) is very similar to those used in two-mode squeezing experiments [41–45], the absence of a well-defined phase reference associated to the noisy dc bias V prevents us from using the standard heterodyne techniques to characterize the emitted radiation.

In conclusion we have shown that a dc-biased Josephson junction in series with two resonators provides a simple and bright source of nonclassical radiation, displaying relative fluctuations of the populations of the two modes below the classical limit. We have also presented a theory that quantitatively accounts for our experimental findings. While the present experiment is performed at microwave frequencies using aluminum Josephson junctions, the

physics involved here can be transposed to higher gap superconductors, such as NbTiN or even YBaCuO, opening the possibility of creating nonclassical THz radiations. The device used in the experiments reported here could also be straightforwardly used to implement a quantum thermal machine [46–48].

We gratefully acknowledge partial support from LabEx PALM (Grant No. ANR-10-LABX-0039-PALM), ANR Contracts No. ANPhoTeQ and No. GEARED, the ERC through the NSECPROBE Grant No. 639039, IQST, and the German Science Foundation (DFG) through Grant No. AN336/11-1.

*Present address: CEA, INAC-SPSMS, F-38000 Grenoble, France.
†joachim.ankerhold@uni-ulm.de
‡fabien.portier@cea.fr

[1] R. J. Glauber, Phys. Rev. **131**, 2766 (1963).
[2] R. J. Schoelkopf, P. J. Burke, A. A. Kozhevnikov, D. E. Prober, and M. J. Rooks, Phys. Rev. Lett. **78**, 3370 (1997).
[3] E. Zakka-Bajjani, J. Ségala, F. Portier, P. Roche, D. C. Glattli, A. Cavanna, and Y. Jin, Phys. Rev. Lett. **99**, 236803 (2007).
[4] G. Gasse, C. Lupien, and B. Reulet, Phys. Rev. Lett. **111**, 136601 (2013).
[5] O. Astafiev, K. Inomata, A. O. Niskanen, T. Yamamoto, Y. A. Pashkin, Y. Nakamura, and J. S. Tsai, Nature (London) **449**, 588 (2007).
[6] Y.-Y. Liu, K. D. Petersson, J. Stehlik, J. M. Taylor, and J. R. Petta, Phys. Rev. Lett. **113**, 036801 (2014).
[7] Y.-Y. Liu, J. Stehlik, C. Eichler, M. J. Gullans, J. M. Taylor, and J. R. Petta, Science **347**, 285 (2015).
[8] F. Chen, J. Li, A. D. Armour, E. Brahimi, J. Stettenheim, A. J. Sirois, R. W. Simmonds, M. P. Blencowe, and A. J. Rimberg, Phys. Rev. B **90**, 020506 (2014).
[9] M. C. Cassidy, A. Bruno, S. Rubbert, M. Irfan, J. Kammhuber, R. N. Schouten, A. R. Akhmerov, and L. P. Kouwenhoven, Science **355**, 939 (2017).
[10] C. W. J. Beenakker and H. Schomerus, Phys. Rev. Lett. **86**, 700 (2001).
[11] C. W. J. Beenakker and H. Schomerus, Phys. Rev. Lett. **93**, 096801 (2004).
[12] I. C. Fulga, F. Hassler, and C. W. J. Beenakker, Phys. Rev. B **81**, 115331 (2010).
[13] A. V. Lebedev, G. B. Lesovik, and G. Blatter, Phys. Rev. B **81**, 155421 (2010).
[14] F. Hassler and D. Otten, Phys. Rev. B **92**, 195417 (2015).
[15] A. D. Armour, M. P. Blencowe, E. Brahimi, and A. J. Rimberg, Phys. Rev. Lett. **111**, 247001 (2013).V. Gramich, B. Kubala, S. Rohrer, and J. Ankerhold, Phys. Rev. Lett. **111**, 247002 (2013).
[16] J. Leppäkangas, M. Fogelström, A. Grimm, M. Hofheinz, M. Marthaler, and G. Johansson, Phys. Rev. Lett. **115**, 027004 (2015).
[17] M. J. Gullans, J. Stehlik, Y.-Y. Liu, C. Eichler, J. R. Petta, and J. M. Taylor, Phys. Rev. Lett. **117**, 056801 (2016).
[18] D. Averin, Y. Nazarov, and A. Odintsov, Physica (Amsterdam) **165–166B**, 945 (1990).
[19] G.-L. Ingold and Y. V. Nazarov, in *Single Charge Tunneling*, edited by H. Grabert and M. H. Devoret (Plenum, New York, 1992).
[20] T. Holst, D. Esteve, C. Urbina, and M. H. Devoret, Phys. Rev. Lett. **73**, 3455 (1994).
[21] J. Basset, H. Bouchiat, and R. Deblock, Phys. Rev. Lett. **105**, 166801 (2010).
[22] M. Hofheinz, F. Portier, Q. Baudouin, P. Joyez, D. Vion, P. Bertet, P. Roche, and D. Esteve, Phys. Rev. Lett. **106**, 217005 (2011).
[23] J. Basset, H. Bouchiat, and R. Deblock, Phys. Rev. B **85**, 085435 (2012).
[24] See Supplemental Material http://link.aps.org/supplemental/10.1103/PhysRevLett.119.137001 for a general predictions for $g(2)$, the basic rate-equation model, the dynamics of the correlation functions, the description of the microwave chain, the mean power measurements, the characterization of the microwave resonators, the high bias shot noise data, and the power fluctuations measurement.
[25] More specifically, to keep stimulated emission effects negligible, one must ensure that the number of photons is well below $1/\Delta_{a,b}^2$ with $\Delta_{a,b} = (2e^2 Z_{a,b}/\hbar)^{1/2}$.
[26] A. D. Armour, B. Kubala, and J. Ankerhold, Phys. Rev. B **91**, 184508 (2015).
[27] M. Trif and P. Simon, Phys. Rev. B **92**, 014503 (2015).
[28] J. Leppäkangas, G. Johansson, M. Marthaler, and M. Fogelström, Phys. Rev. Lett. **110**, 267004 (2013).
[29] T. Debuisschert, S. Reynaud, A. Heidmann, E. Giacobino, and C. Fabre, Quantum Opt. **1**, 3 (1989).
[30] A. Heidmann, R. J. Horowicz, S. Reynaud, E. Giacobino, C. Fabre, and G. Camy, Phys. Rev. Lett. **59**, 2555 (1987).
[31] G. Brida, L. Caspani, A. Gatti, M. Genovese, A. Meda, and I. R. Berchera, Phys. Rev. Lett. **102**, 213602 (2009).
[32] J.-C. Forgues, C. Lupien, and B. Reulet, Phys. Rev. Lett. **113**, 043602 (2014).
[33] We determine the response time of the quadractic detectors by measuring the spectral density of the fluctuations of their output voltage as a consequence of the fluctuations of the noise power of the amplifiers. More details on this point can be found in Supplemental Material.
[34] J. Gabelli, L.-H. Reydellet, G. Fève, J.-M. Berroir, B. Plaçais, P. Roche, and D. C. Glattli, Phys. Rev. Lett. **93**, 056801 (2004).
[35] E. Zakka-Bajjani, J. Dufouleur, N. Coulombel, P. Roche, D. C. Glattli, and F. Portier, Phys. Rev. Lett. **104**, 206802 (2010).
[36] D. Bozyigit, C. Lang, L. Steffen, J. M. Fink, C. Eichler, M. Baur, R. Bianchetti, P. J. Leek, S. Filipp, M. P. da Silva *et al.*, Nat. Phys. **7**, 154 (2011).
[37] I.-C. Hoi, T. Palomaki, J. Lindkvist, G. Johansson, P. Delsing, and C. M. Wilson, Phys. Rev. Lett. **108**, 263601 (2012).
[38] J. Goetz, S. Pogorzalek, F. Deppe, K. G. Fedorov, P. Eder, M. Fischer, F. Wulschner, E. Xie, A. Marx, and R. Gross, Phys. Rev. Lett. **118**, 103602 (2017).
[39] Note that in practice, due to the necessity of refilling the helium vessel between two measurement points, which induces a variation of the flux through the SQUID,

$g^{(2)}_{a,a}$, $g^{(2)}_{b,b}$, and $g^{(2)}_{a,b}$ were not always measured at exactly the same pair emission rate. In that case, the NRF was deduced using the measured value of $g^{(2)}_{a,b}$ and extrapolating the value of $g^{(2)}_{a,a}$, $g^{(2)}_{b,b}$ from adjacent points.

[40] J. Leppäkangas, G. Johansson, M. Marthaler, and M. Fogelström, New J. Phys. **16**, 015015 (2014).

[41] N. Bergeal, F. Schackert, L. Frunzio, and M. H. Devoret, Phys. Rev. Lett. **108**, 123902 (2012).

[42] C. Eichler, D. Bozyigit, C. Lang, M. Baur, L. Steffen, J. M. Fink, S. Filipp, and A. Wallraff, Phys. Rev. Lett. **107**, 113601 (2011).

[43] E. Flurin, N. Roch, F. Mallet, M. H. Devoret, and B. Huard, Phys. Rev. Lett. **109**, 183901 (2012).

[44] J.-C. Forgues, C. Lupien, and B. Reulet, Phys. Rev. Lett. **114**, 130403 (2015).

[45] K. G. Fedorov, S. Pogorzalek, U. Las Heras, M. Sanz, P. Yard, P. Eder, M. Fischer, J. Goetz, E. Xie, K. Inomata *et al.*, arXiv:1703.05138.

[46] P. P. Hofer, J.-R. Souquet, and A. A. Clerk, Phys. Rev. B **93**, 041418 (2016).

[47] P. P. Hofer, M. Perarnau-Llobet, J. B. Brask, R. Silva, M. Huber, and N. Brunner, Phys. Rev. B **94**, 235420 (2016).

[48] P. P. Hofer, J. Bohr Brask, M. Perarnau-Llobet, and N. Brunner, Phys. Rev. Lett. **119**, 090603 (2017).